A UNIQUE AMPHIBOLE- AND MAGNETITE-RICH CARBONACEOUS CHONDRITE FROM ALMAHATA SITTA. C. A. Goodrich,[1], V. E. Hamilton[2] , M. Zolensky[3], N. T. Kita[4], A. M. Fioretti[5], I. Kohl[6], E. Young[6], A. H. Treiman[1], H. C. Connolly Jr.[7], J. Filiberto[1], M. H. Shaddad[8], and P. Jenniskens[9]. [1]Lunar & Planetary Institute, USRA, Houston, TX 77058 USA, goodrich@lpi.usra.edu; [2]Southwest Research Institute, Boulder, CO 80302 USA; [3]ARES, NASA-JSC, Houston TX 77058 USA; [4]WiscSIMS, Dept. Geoscience, Univ. of Wisconsin, Madison, WI 53706 USA; [5]CNR–Istituto di Geoscienze e Georisorse, I-35131 Padova, Italy; [6]UCLA, Los Angeles CA 90095 USA; [7]Rowan University, Glassboro, NJ 08028 USA. [8]Dept. Astronomy, Univer. of Khartoum, Khartoum, 11115 Sudan; [9]SETI Institute, Mountain View, CA 94043 USA.

Introduction: Almahata Sitta (AhS) 202 from the UoK collection [1] represents a clast from the polymict breccia asteroid 2008 TC_3 [2-4]. AhS 202 was recognized as a unique carbonaceous chondrite (CC) with a high magnetite content [5-7]. Here we report that it also contains a significant amount of amphibole, a mineral that is very rare in chondrites [8,9] and has not previously been reported in significant abundance in a CC [10,11]. We present new petrographic, oxygen isotope, and micro-FTIR [see 12] data. We discuss petrogenesis and possible relationships to known CC.

Sample: Almahata Sitta (AhS) 202 had an original mass of 20.057 g [1]. We were allocated <50 mg from which we prepared a polished mount (area ~8.8 mm^2) and a small chip for bulk oxygen isotope analyses.

Methods: Electron imaging, X-ray mapping, and electron microprobe analyses (EMPA) were conducted at ARES, JSC. Bulk oxygen isotope analyses were obtained at UCLA. Oxygen isotope analyses of minerals were obtained by secondary ion mass spectrometry (SIMS) at WiscSIMS. Micro-FTIR spectroscopy was conducted at SwRI [12].

Petrography and Mineral Compositions: AhS 202 has a chondritic texture of altered or partially altered chondrules (up to 700 μm diameter) in a completely altered matrix (Fig. 1). The chondrules have thick rims of magnetite with included Fe,Ni sulfides (Fig. 1). The interiors of some chondrules contain massive olivine (Fig. 1a), as well as texturally complex assemblages of amphibole, diopside, serpentine, and other alteration phases. Other chondrules have completely altered interiors (Fig. 1b). There are also spherules of magnetite (up to ~450 μm diameter) that may themselves be chondrules and have inclusions of (apatite and Fe,Ni sulfides. The matrix is similar to the alteration assemblages in the chondrules.

The composition of the olivine (37 analyses) is Fa 32.2±0.4, 0.03±0.01 wt.% Cr_2O_3, ~0.1±0.2 wt.% NiO and 1.3±0.1 wt.% MnO. Magnetite occurs as massive rims around chondrules (Fig. 1,2), euhedral/subhedral grains (or clusters thereof), and framboids. Its composition (0.30-0.65 wt.% TiO_2, 0.09-3.3 wt.% Cr_2O_3, ≤0.06 wt.% Al_2O_3, 0.25-1.24 wt.% MgO; 45 analyses) is unique compared with compositions of magnetite in CK, CV, CR and CI (Fig. 2).

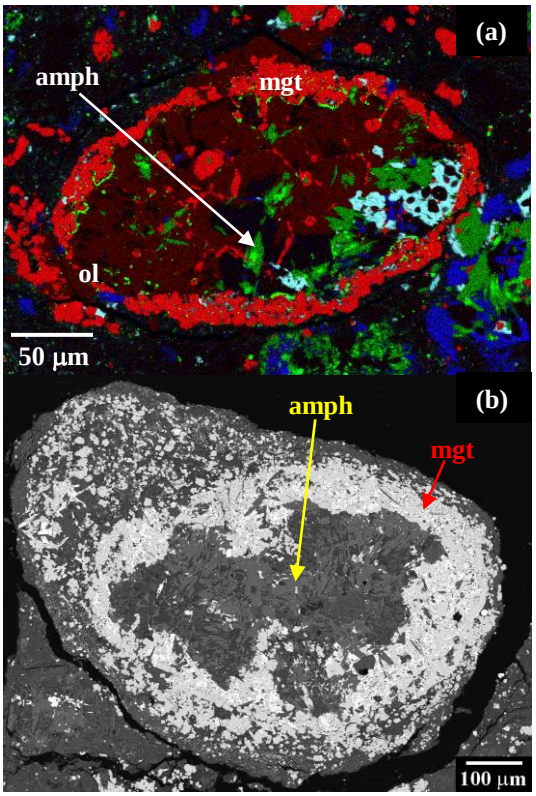

Fig. 1. Chondrules in AhS 202. (a) Fe (red), Ca (green), Al (blue), S (cyan) X-ray map. Chondrule interior contains massive olivine (ol) plus alteration phases including amphibole (green) (amph). Chondrule rim consists of magnetite (red) (mgt) with included Fe,Ni sulfides. (b) Back-scattered electron image (BEI). Chondrule interior consists entirely of alteration phases including abundant amphibole.

Using Micro-FTIR spectroscopy we identified the presence and composition of amphibole. Details are provided by [12], with preliminary spectral results suggesting a *minimum* of 5 vol% in the fragment. The amphibole occurs as prismatic and bladed crystals and fibrous aggregates (Fig. 1,2). EMPA confirms that it is nearly endmember tremolite (tr). The average formula normalized to 15 cations [13] is:

$(\square_{0.81},Na_{0.19})_{1.0}(Ca_{1.86},Fe_{0.14})_{2.0}(Mg_{4.62},Fe^{2+}_{0.34},Mn_{0.02},Cr_{0.01})_{4.99}(Si_{7.96}Al_{0.04})_{8.0}O_{22}[(O^{2-})_{0.18},(OH)_{1.82}]_{2.0}$

A 13 cation normalization [14] gives:

$(\square_{0.97}Na_{0.03})_{1.0}(Ca_{1.84},Na_{0.16})_{2.0}(Mg_{4.58},Fe^{2+}_{0.16},Fe^{3+}_{0.24},Mn_{0.02})_{5.0}(Si_{7.88}Al_{0.04},Fe^{3+}_{0.08})_{8.0}O_{22}(OH)_{2.0}$

Diopside (di) occurs in a patchy texture on amphibole crystals or less commonly as prismatic crystals (Fig. 3). At least three other phases are present. Mg-rich (Mg# 86-92) serpentine (ser) occurs as fibrous crystals. An aluminous phase (11-12 wt.% Al_2O_3) with lamellar or fibrous texture might be a septochlorite or chlorite/serpentine intergrowth (Fig. 3). A pervasive interstitial phase might be Mg-Fe smectite (Fig. 3).

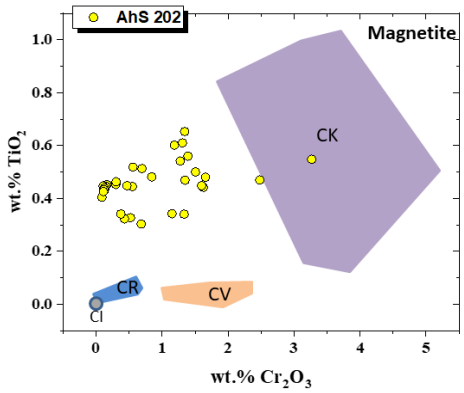

Fig. 2. Wt.% Cr_2O_3 and TiO_2 in magnetite in AhS 202, compared with magnetite in CI, CR, CV and CK [16-21].

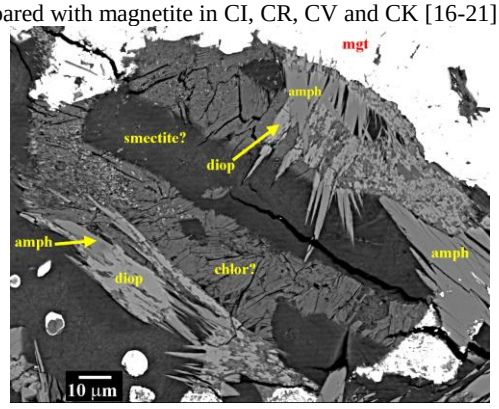

Fig. 3. BEI of some alteration minerals in AhS 202 showing amphibole (amph)-diopside (diop) reaction textures and tentatively identified septochlorite (chlor?) and smectite (?).

Oxygen Isotopes: The bulk composition of AhS 202 plots near the CCAM line with $\Delta^{17}O$ = -1.73±0.01, at the intersection of fields for CV, CM, and CR (Fig. 4). Compositions of magnetite, olivine and amphibole plot along a regression of slope 0.60±0.12 and intercept -1.8±0.5, consistent with a mass fractionation line through the bulk. SIMS data for amphibole were calculated using a pyroxene standard, due to the lack of an amphibole standard. This will be rectified in the future. The olivine-magnetite fractionation temperature was calculated to be 330(+230/-110)˚C.

Metamorphism: The minerals in AhS 202 are related by: 2 di + 5 ser = tr + 6 ol + 9 H_2O. The P-T curve of this reaction was determined, using analyzed mineral compositions, from the THERMOCALC 3.50 and AX62 programs [15]. If T was <400C°, then P_{H2O}<0.5 kbar. If T was >450°C, then P_{H2O} >4 kbar.

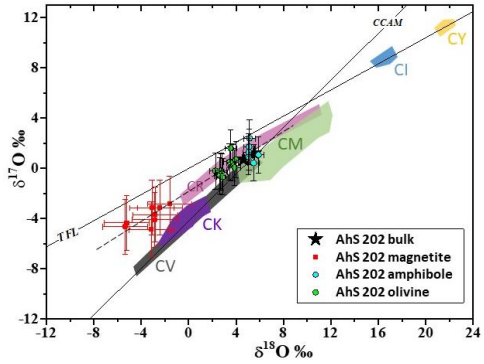

Fig. 4. Oxygen isotope compositions for AhS 202. Dashed line is a regression through the mineral data.

Discussion: The presence of abundant amphibole in AhS 202 makes it unique and indicates that it experienced hydrous metamorphic conditions unlike other CC. Nevertheless, it may have been derived from precursor materials similar to those of known CC. Bulk oxygen isotopes suggest CM, CR or CV as possibilities (not CK, despite the similarly high magnetite contents). Magnetite compositions are not consistent with CV or CR but may have been altered by metamorphism.

Petrogenesis: Although many CC have experienced aqueous alteration that produced magnetite and phyllosilicates (serpentine and smectites), formation of abundant amphibole (and chlorite) in relatively coarse grains as in AhS 202 requires longer metamorphic durations and more abundant water. The relatively high P_{H2O} required suggests formation in a single, prograde alteration/metamorphic sequence on a large, water-rich CC asteroid [e.g., 8,22]. Alternatively, an aqueously altered CC lithology may have been re-heated by impact with re-mobilization of water.

References: [1] Shaddad M.H. et al. 2010. *MAPS* 45, 1618–1637. [2] Jenniskens P. et al. 2009. *Nature* 458, 485–488. [3] Horstmann M. & Bischoff A. 2014. *Chemie der Erde* 74, 149-183. [4] Goodrich C.A. et al. 2015. *MAPS* 50, 782-809. [5] Fioretti A.M. et al. 2017. *LPSC* 48, #1846. [6] Goodrich C.A. et al. 2018. *LPSC* 49, #1321. [7] Kita N.T. et al. 2019. *LPSC* 50, #1551 [8] McCanta M. et al. 2008. *GCA* 72, 5757-5780. [9] Rubin A.E & Ma C. 2017. *Chemie der Erde 77*, 325-385. [10] Brearley A.J. 1997. *Science*, *276*, 1103-1105. [11] Dobrica E. & Brearley A.J. 2014. *MAPS* 49, 1323-1349. [12] Hamilton V.E. et al. 2020. *LPSC* 51, #1230. [13] Giesting P. & Filiberto J. 2014. *Am. Min.* 99, 852-865. [14] Leake B.E. et al. 1997. *Europ. J. Mineral.* 9 623-651. [15] Green E.C.R. et al. 2016. *J. Metam. Geol.* 34, 845-892. [16] Greenwood R.C. et al. 2010. *GCA* 74, 1684-1705. [17] Chaumard N. et al. 2014. *MAPS* 49, 419-452. [18] Wasson J. et al. 2013. *GCA* 108, 45-63. [19] Dunn T.L. et al. 2016. *MAPS* 51, 1701-1720. [20] Davidson J. et al. 2014. *MAPS* 49, 1456-1474. [21] Harju E. R. et al. 2014 *GCA* 139, 267-292. [22] Gross J. et al. 2017. *MAPS* 52(S1), # 6145.